

1 **Title Page**

2 **Title:** Detection of SARS-CoV-2 RNA Throughout Wastewater Treatment Plants and  
3 A Modeling Approach to Understand COVID-19 Infection Dynamics in Winnipeg,  
4 Canada

5 **Author's names:** Kadir Yanaç<sup>1</sup>, Adeola Adegoke<sup>2</sup>, Liqun Wang<sup>2</sup>, Qiuyan Yuan<sup>1</sup>  
6 Miguel Uyaguari<sup>3</sup>

7 <sup>1</sup> Department of Civil Engineering, University of Manitoba, Winnipeg, Manitoba,  
8 Canada

9 <sup>2</sup> Department of Statistics, University of Manitoba, Winnipeg, Manitoba, Canada

10 <sup>3</sup> Department of Microbiology, University of Manitoba, Winnipeg, Manitoba, Canada

11

12

13

14

15

16

17

18

19

20

21 **NOTE:** This preprint reports new research that has not been certified by peer review and should not be used to guide clinical practice.

22  
23  
24  
25  
26  
27  
28  
29  
30  
31  
32  
33  
34  
35  
36  
37  
38  
39  
40  
41  
42  
43  
44  
45  
46

## ABSTRACT

*Although numerous studies have detected SARS-CoV-2 in wastewater and attempted to find correlations between the concentration of SARS-CoV-2 and the number of cases, no consensus has been reached on sample collection and processing, and data analysis. Moreover, the fate of SARS-CoV-2 in wastewater treatment plants is another issue, specifically regarding the discharge of the virus into environmental settings and the water cycle. The current study monitored SARS-CoV-2 in influent and effluent wastewater samples with three different concentration methods and sludge samples over six months (July to December 2020) to compare different virus concentration methods, assess the fate of SARS-CoV-2 in wastewater treatment plants, and describe the potential relationship between SARS-CoV-2 concentrations in influent and infection dynamics. Skimmed milk flocculation (SMF) resulted in higher recoveries ( $15.27\% \pm 3.32\%$ ) of an internal positive control, Armored RNA, and higher positivity rate of SARS-CoV-2 in samples compared to ultrafiltration methods employing a prefiltration step to eliminate solids. Our results suggested that SARS-CoV-2 may predominate in solids and therefore, concentration methods focusing on both supernatant and solid fractions may result in better recovery. SARS-CoV-2 was detected in influent and primary sludge samples but not in secondary and final effluent samples, indicating a significant reduction during primary and secondary treatments. SARS-CoV-2 was first detected in influent on September 30<sup>th</sup>, 2020. A decay-rate formula was applied to estimate initial concentrations of late-processed samples with SMF. A model based on shedding rate and new cases was applied to estimate SARS-CoV-2 concentrations and the number of active shedders. Inferred sensitivity of observed and modeled concentrations to the fluctuations in new cases and test-positivity rates indicated a*

47 *potential contribution of newly infected individuals to SARS-CoV-2 loads in*  
48 *wastewater.*

## 49 1. Introduction

50 After the initial emergence of COVID-19 in December 2019 in Wuhan, China, the  
51 disease has rapidly spread and caused significant health, economic and social  
52 burden worldwide. Considering the rapid transmission and spread of COVID-19 and  
53 the subsequent emergence of new waves and variants, surveillance of the disease is  
54 vital to early predict and control outbreaks in communities. Standard diagnostic  
55 testing among populations is challenging due to the time and cost to test massive  
56 numbers of individuals. Moreover, undiagnosed and unreported asymptomatic and  
57 mildly symptomatic cases of COVID-19 constitute a significant proportion of  
58 infections (Bi et al., 2021; Day, 2020; Ing et al., 2020), and this increases the  
59 complexity of assessing the true scale of a community outbreak. With the first  
60 detection of SARS-CoV-2 in urban wastewater reported in the Netherlands in March  
61 2020, when number of cases were very low (and even zero in some locations  
62 (Medema et al., 2020a)), wastewater-based epidemiology (WBE) has emerged as an  
63 additional surveillance tool to mitigate these challenges and provide rapid information  
64 to government agencies, civil society organizations, and private or public utilities to  
65 determine the effectiveness of public health control measures and the required level  
66 of societal restrictions (Bivins et al., 2020b; Hill et al., 2020; Thompson et al., 2020).  
67 Moreover, the existence of SARS-CoV-2 in wastewater treatment plants (WWTPs) is  
68 concerning because of its health risks to the workers and its potential dissemination  
69 into the environment through discharge.

70 WBE has been used as a surveillance and predictive tool to provide real-time  
71 information on the usage of illegal drugs (Bishop et al., 2020; Sulej-Suchomska et al.,

72 2020), and the prevalence of viral (Bisseux et al., 2018; Ivanova et al., 2019; McCall  
73 et al., 2020; Nakamura et al., 2015) and bacterial (Diemert and Yan, 2020; Yan et al.,  
74 2018) diseases. Presence of SARS-CoV-2 gene fragments in the feces of both  
75 symptomatic and asymptomatic infected individuals (Gupta et al., 2020; Jones et al.,  
76 2020; Pan et al., 2020) makes wastewater surveillance of COVID-19 a unique  
77 epidemiological tool to monitor infection trends in communities and support public  
78 health interventions. Indeed, since the onset of COVID-19, many researchers have  
79 reported the detection and quantitation of SARS-CoV-2 in wastewater (Ahmed et al.,  
80 2020a; D'Aoust et al., 2021; Graham et al., 2021; Medema et al., 2020a; Westhaus et  
81 al., 2021). Several potential uses of the generated data include tracking trends  
82 temporally to project future infection trajectories (Medema et al., 2020b) and  
83 estimating COVID-19 prevalence in a community based on SARS-CoV-2  
84 concentration in wastewater (Ahmed et al., 2020a; Gerrity et al., 2021; Wu et al.,  
85 2022). Moreover, surveillance of primary sewage sludge and wastewater solids,  
86 specifically the partition of enveloped viruses to the wastewater solids (Ye et al.,  
87 2016), has also been reported as an alternative to wastewater influent surveillance  
88 (Graham et al., 2021; Peccia et al., 2020). In fact, processing sludge and solids  
89 samples using reverse-transcriptase quantitative polymerase chain reaction (RT-  
90 qPCR) (Peccia et al., 2020) is not as labor-intensive as processing wastewater  
91 influent samples, in which viral particles are concentrated either using filtration  
92 methods or organic flocculation methods (Ahmed et al., 2020c; Barril et al., 2021).  
93 However, regardless of the surveillance type, there are still some methodological  
94 questions on the cumulative interpretation of data generated from wastewater  
95 analysis and epidemiological data together.

96 Our knowledge of the fate of coronaviruses in environmental compartments is very  
97 limited (Carducci et al., 2020). Westhaus et al. (2021) detected SARS-CoV-2 in  
98 treated wastewater, indicating its potential distribution into aquatic ecosystems, while  
99 Hasan et al. (2021) could not detect SARS-CoV-2 in treated wastewater. Detection of  
100 SARS-CoV-2 in wastewater solids and sludge (Balboa et al., 2020; D'Aoust et al.,  
101 2021; Graham et al., 2021; Peccia et al., 2020) might indicate the predominance of  
102 SARS-CoV-2 in solids and sludge line as the primary removal mechanism in  
103 WWTPs. Thus, concentration methods focusing on the recovery from both solids and  
104 supernatant may better approach the true concentrations of SARS-CoV-2 in  
105 wastewater (Chik et al., 2021). Different wastewater treatment processes, sewage  
106 characteristics, and climate conditions may affect the fate of SARS-CoV-2 in  
107 WWTPs. More in-depth investigations will provide better insights into the fate of  
108 SARS-CoV-2 throughout WWTPs and its circulation in the water cycle.

109 This study monitored SARS-CoV-2 concentrations using raw composite wastewater  
110 samples from three WWTPs in Winnipeg over six months (July to December 2020),  
111 characterized by increasing COVID-19 incidence and prevalence. We applied three  
112 different concentration methods to process raw wastewater samples. SARS-CoV-2  
113 concentrations in raw wastewater were analyzed for the population-wide infection  
114 dynamics in Winnipeg. We used a back trajectory modeling approach to estimate the  
115 initial concentration of SARS-CoV-2 genes in the late processed wastewater  
116 samples. A second model was also applied to estimate the concentration of SARS-  
117 CoV-2 based on reported cases and shedding rate. Furthermore, we also monitored  
118 SARS-CoV-2 concentrations in the effluent and primary sludge samples to  
119 understand the fate of SARS-CoV-2 in WWTPs.

## 120 2. Materials and Methods

## 121 2.1. Sample Collection

122 One-liter of 24-h composite raw wastewater samples were collected from three major  
123 WWTPs in Winnipeg, Canada, between July 8 and December 15, 2020. These  
124 WWTPs are the North End Sewage Treatment Plant (NESTP), South End Sewage  
125 Treatment Plant (SESTP), and West End Sewage Treatment Plant (WESTP).  
126 Primary sludge (50 mL), secondary effluent (1 L), and final effluent (1 L) samples  
127 were also collected during this period. Detailed information on sampling dates,  
128 sample types, and treatment processes of WWTPs and their design capacities is  
129 provided in Table S1 and Table S2, respectively. The operators provided daily  
130 flowrate (Fig. S1) and wastewater characteristics data. Wastewater and sludge  
131 samples were transported to the laboratory in amber HDPE bottles in an icebox after  
132 sampling and processed within 24 hours.

## 133 2.2. Virus Concentration Assays

134 Three different virus concentration methods were applied: an ultrafiltration method at  
135 two different centrifugation speeds and an organic flocculation method.

### 136 *Ultrafiltration*

137 Samples were processed within 24 hours of collection. Raw wastewater, and  
138 secondary and final effluent samples (120 mL each) were filtered through  
139 cheesecloth and low-protein binding 0.45 and 0.2  $\mu\text{m}$  47-mm Supor-200 membrane  
140 disc filters (Pall Corporation, Ann Harbor, MI), respectively, to remove large particles,  
141 sediments, eukaryotes, and bacteria (Uyaguari-Diaz et al., 2016). Solids retained on  
142 the filters were stored at  $-20\text{ }^{\circ}\text{C}$ .

143 *Sequential ultrafiltration at 3000g (UF-3K x g)*: A total of 120 mL of the sample was  
144 first concentrated, at 3000 g for 30 minutes by loading 60 mL of the sample twice, to

145 approximately 5 mL using Jumbosep Centrifugal Device, 30-kDa (Pall Corporation,  
146 Ann Harbor, MI, USA). Then, the 5 mL concentrate was further concentrated down at  
147 3000 g for 30 minutes using Microsep Advance Centrifugal Device, 30-kDa, (Pall  
148 Corporation, Ann Harbor, MI, USA). The final volume of the concentrate varied  
149 between 500 and 1200  $\mu$ L.

150 *Sequential ultrafiltration at 7500g (UF-7.5K x g)*: To get smaller final volumes and as  
151 per the manufacturer's recommendation, centrifugation speed for Microsep was  
152 changed from 3000 g to 7500 g from October 28<sup>th</sup>, 2020.

153 Samples collected between October 28<sup>th</sup> and December 15<sup>th</sup> were processed with  
154 both UF-3K x g and UF-7.5K x g methods.

#### 155 *Organic Flocculation*

156 The samples collected between November 16<sup>th</sup> and December 15<sup>th</sup> were additionally  
157 concentrated by applying skimmed milk flocculation (SMF) protocol (Calgua et al.,  
158 2008) even though a long time (Table 1) had passed since the sample collection.  
159 Briefly, 0.5 g of skim milk powder (Difco Laboratories, Sparks, MD, USA) was  
160 dissolved in 50 mL synthetic seawater (Sigma-Aldrich, St. Louis, MO, USA) to obtain  
161 1% (w/v) skimmed milk solution and pH of the solution was carefully adjusted with 1M  
162 HCl to 3.5. Five mL of skimmed milk solution was added to 500 mL raw wastewater  
163 samples. pH of samples was also previously adjusted to 3.5 with 1M HCl to obtain a  
164 final concentration of skimmed milk at 0.01% (w/v). Samples were stirred for eight  
165 hours, and flocs were allowed to settle for another eight hours at room temperature.  
166 Supernatants were carefully removed using serological pipets without disturbing the  
167 settled flocs. A final volume of 50 mL containing the flocs was transferred to  
168 centrifuge tubes and centrifuged at 8000 x g for 30 minutes. Pellets were carefully

169 scraped using a sterilized spatula, and the remaining pellets in the tubes were  
170 resuspended in 250  $\mu$ L of 0.2M sodium phosphate buffer with a pH 7.5 (Alfa Aesar,  
171 Ottawa, ON, Canada) and transferred to 1.5 mL Eppendorf tubes.

172 *Recovery Efficiency:* Total recovery for ultrafiltration and SMF method workflows  
173 were determined by spiking  $5 \times 10^4$  copies of Armored RNA Quant IPC-1 Processing  
174 Control (Asuragen, Austin, TX, USA) (Alygizakis et al., 2021; Eveleigh et al., 2019;  
175 Hietala and Crossley, 2006) into six raw wastewater samples from North End  
176 Sewage Treatment Plant (NESTP), South End Sewage Treatment Plant (SESTP)  
177 and West End Sewage Treatment Plant (WESTP) in Winnipeg for each virus  
178 concentration method and then stirring and inoculating the samples at 4°C for 30  
179 minutes. Recovery efficiency percentage was calculated by dividing the recovered  
180 concentration by the spiked concentration.

### 181 2.3. Viral RNA Extraction

182 Viral concentrates from wastewater samples and recovery efficiency assays were  
183 processed using the RNeasy PowerMicrobiome Kit (Qiagen Sciences, Inc.,  
184 Germantown, MD, USA). Phenol:Chloroform: Isoamyl Alcohol 25:24:1 (Invitrogen,  
185 Carlsbad, CA, USA) and  $\beta$ -mercaptoethanol (Fisher Scientific, Fair Lawn, NJ, USA)  
186 were also added during extraction according to the manufacturer's instructions to  
187 improve extraction efficiency. 300  $\mu$ L of sludge samples were added directly to the  
188 beading tubes to extract viral RNA from sludge using the same extraction kit and  
189 following the same instructions. Finally, RNA was eluted in 50  $\mu$ L of elution buffer. On  
190 the other hand, viral RNA was extracted from wastewater solids using MagMAX  
191 Microbiome kit (Thermo Fisher, Waltham, MA, USA) following the manufacturer's  
192 instructions that included the addition of Proteinase K. The RT-qPCR analysis was  
193 conducted following the extraction, and extracts were stored at -80 °C.



## 194 2.4. RT-qPCR Analysis

195 In this study, N1 and N2 primers/probe sets (Integrated DNA Technologies, Inc.,  
196 Coralville, IA, USA), each targeting a different region of the Nucleocapsid (N) gene of  
197 SARS-CoV-2 (CDC, 2020), were used. Each 10- $\mu$ l RT-qPCR mixture consisted of 10  
198  $\mu$ l of 2.5  $\mu$ L of 4X TaqMan Fast Virus 1-Step Master Mix (Life Technologies,  
199 Carlsbad, CA, USA), 400 nM each primer, 250 nM probe, 2.5  $\mu$ l of the template and  
200 ultrapure DNase/RNase free distilled water (Promega Corporation, Fitchburg, WI,  
201 USA). Calibration curves for quantifying N1 and N2 specific assays were obtained  
202 using six 10-fold dilutions (ranging from 2.0 to 2.0E+05) of the 2019-  
203 nCoV\_N\_Positive Control plasmid DNA (Integrated DNA Technologies, Inc.,  
204 Coralville, IA, USA). Armored RNA was quantified using 10-fold dilutions of synthetic  
205 single-stranded DNA (Integrated DNA Technologies, Inc., Coralville, IA, USA).  
206 Primers and probe sets (Integrated DNA Technologies, Inc., Coralville, IA, USA) used  
207 to detect and quantify the Armored RNA are given in Table S3. Calibration curves  
208 were obtained for each RT-qPCR run. Negative controls were also included in each  
209 qPCR run. Thermal cycling reactions were performed at 50 °C for 5 minutes, followed  
210 by 45 cycles of 95 °C for 10 seconds and 60 °C for 30 seconds on a QuantStudio 5  
211 Real-Time PCR System (Life Technologies, Carlsbad, CA, USA). Following  
212 recommendations by the CDC's protocol for detection of SARS-CoV-2 (2020) if the  
213  $C_T$  was <40, samples were considered SARS-CoV-2 positive.

214 The concentration of SARS-CoV-2 in wastewater in Winnipeg was normalized by  
215 dividing daily total SARS-CoV-2 load in wastewater by the total daily wastewater flow  
216 rate (eqn. 1). The normalization was implemented for the three WWTPs using eqn. 1,  
217 where NC is normalized concentration, C represents the SARS-CoV-2 concentration,  
218 and WF indicates the daily wastewater flow.

$$219 \quad NC = \frac{C \text{ at NESTP} \times WF \text{ to NESTP} + C \text{ at SESTP} \times WF \text{ to SESTP} + C \text{ at WESTP} \times WF \text{ to WESTP}}{\text{Sum of WF to NESTP, SESTP, WESTP}} \quad \text{eqn. 1}$$

## 220 2.5. Model 1: Back Trajectory Modeling

221 We used SMF to concentrate SARS-CoV-2 from the raw wastewater samples stored  
222 at 4 °C. The delay times in sample processing with SMF approach are provided in  
223 Table 1.

224 **Table 1.** Delay in sample processing collected from NESTP, SESTP, and WESTP

225 Sampling date	Delay in sample processing (days)
November 16, 2020	75
November 18, 2020	73
December 1, 2020	60
December 8, 2020	53
December 15, 2020	46

226 To estimate the initial concentration of SARS-CoV-2 genes on the sampling day, a  
227 model was derived based on the previously reported decay rate constants for N1  
228 (Ahmed et al., 2020b) and N2 (Hokajärvi et al., 2021a) genes at 4 °C in untreated  
229 wastewater (Table 2). Both Ahmed et al. (2020b) and Hokajärvi et al. (2021a)  
230 linearized the observed RNA concentrations using the natural logarithm (ln)-  
231 transformation of the normalized concentrations (eqn. 2). The decay rate (k) for N2  
232 was re-calculated as 0.063 (R<sup>2</sup>=0.99) in units per day by linear regression using the  
233 data reported by Hokajärvi et al. (2021a), while the decay rate (k) reported by Ahmed  
234 et al. (2020b) was used for N1 assay.

$$235 \quad \ln\left(\frac{C_t}{C_0}\right) = -k * t \quad \text{eqn. 2}$$

236 Where  $C_t$  is the concentration at time  $t$ ,  $C_0$  represents the initial concentration, and  $k$   
 237 indicates the decay rate. A log-linear model was derived from eqn. 2 for the back-  
 238 calculation of N1 and N2 concentrations (gene copies) as shown in eqn. 3, where  $C_t$   
 239 is the concentration of N1 or N2 genes at time  $t$ ,  $C_0$  is the initial concentration of N1  
 240 or N2 genes at the sampling day,  $k$  is the decay rate of N1 or N2 genes, and  $t$  is the  
 241 delay in processing the samples.

242 
$$C_0 = \frac{C_t}{e^{-k \cdot t}} \quad \text{eqn. 3}$$

243 **Table 2.** Reported decay rate characteristics of the SARS-CoV-2 in untreated  
 244 wastewater at 4°C

Assay	Decay rate (k)	R <sup>2</sup>	T <sub>50</sub> (days)	T <sub>90</sub> (days)	T <sub>99</sub> (days)	Reference
N1	0.084 ± 0.013	0.79		27.8 ± 4.45		(Ahmed et al., 2020b)
N2	0.06 ± 0.0	0.99	11	36	73	(Hokajärvi et al., 2021a)

245

246 2.6. Model 2: Estimation of Number of Shedding Cases, and SARS-CoV-2  
 247 Concentration

248 The second model was adopted from Gerrity et al. (2021) with slight changes to  
 249 estimate SARS-CoV-2 concentration and number of shedding cases as a function of  
 250 new cases in the city, fecal shedding rate, and daily total wastewater flowrate. The  
 251 model was rewritten in RStudio since the original script was written in MATLAB. This  
 252 model assumes the feces production rate and initial fecal shedding rate are 126  
 253 g/person-d and 10<sup>8.9</sup> GC/g feces with a decay rate 10<sup>0.35</sup> GC/g feces-day, respectively  
 254 (Gerrity et al., 2021; Wölfel et al., 2020). The ascertainment ratio was assumed as 2

255 (Gerrity et al., 2021), which means the model will multiply the number of cases by 2.  
256 Instead of assuming a constant daily wastewater flow rate, we used daily wastewater  
257 flow rates provided by the city of Winnipeg. Based on the shedding rate and  
258 shedding decay rate, an infected person is expected to shed SARS-CoV-2 for 26  
259 days with a burst on the initial days of infection.

## 260 2.7. Epidemiological Data

261 Information regarding new, cumulative and active cases, and test-positivity rates of  
262 COVID-19 was provided by the Manitoba Regional Health Authority (Manitoba,  
263 2021).

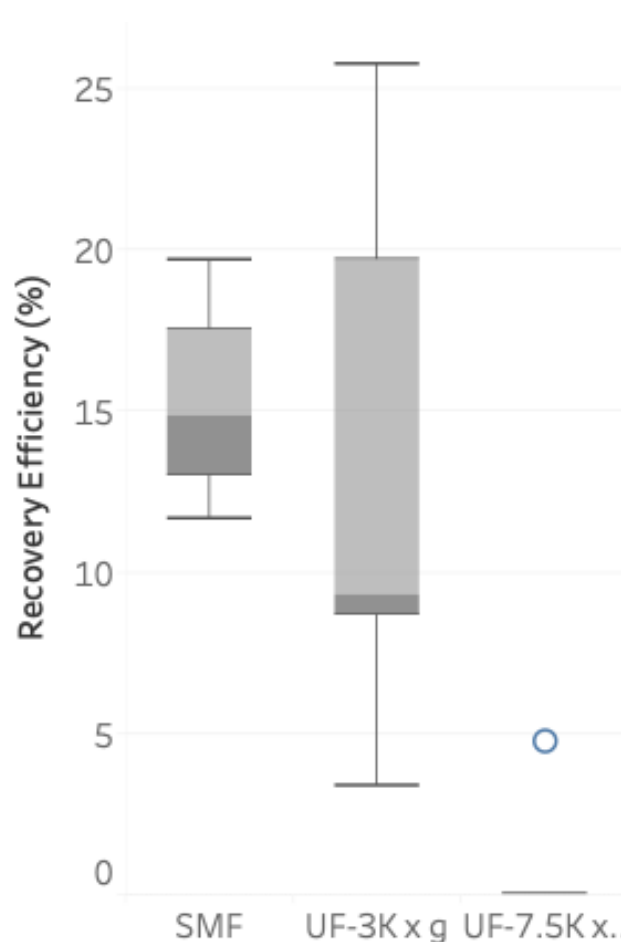
## 264 3. Results and Discussion

### 265 3.1. Evaluation of SARS-CoV-2 concentration methods

266 Viral concentration with UF-3K x g resulted in  $13.38 \pm 9.11$  % recovery (Fig. 1) and a  
267 final volume varying between 500 and 1200  $\mu\text{L}$ . The high standard deviation could be  
268 attributed to the losses between the two-step ultrafiltration process. This two-step  
269 process resulted in high final volumes, which require multiple bead tubes and  
270 additional use of extraction kit solutions for RNA extraction since bead tubes have a  
271 maximum capacity of 300  $\mu\text{L}$  of sample. During extraction, all tubes of the same  
272 sample were eluted into the same spinning column to collect total RNA. The use of  
273 multiple bead tubes can be another reason for the high variability in the recovery  
274 efficiency.

275 To decrease variability in recovery efficiency potentially caused by the use of multiple  
276 bead tubes, the centrifugation speed of Microsep Advance Centrifugal Device was  
277 increased from 3000g to 7500g, which generally resulted in final volume less than  
278 400  $\mu\text{L}$ . The first trial with UF-7.5K x g resulted in 4.79% recovery of Armored RNA

279 (Fig. 1). After getting negative or weak SARS-CoV-2 genetic signals in wastewater  
280 samples with UF-7.5K x g, further recovery experiments were conducted to  
281 determine recovery efficiency at 7500 x g, and but Armored RNA was not recovered.  
282 Apparently, increasing the centrifugation speed impacted the recovery, probably  
283 caused Armored RNA to pass through or bind onto the filters. Filtration with  
284 cheesecloth and low-protein binding 0.45 and 0.2  $\mu\text{m}$  47-mm membrane filters before  
285 ultrafiltration might also be another reason for no detection and weak signals of  
286 SARS-CoV-2 due to the elimination of solid particles, which could carry a significant  
287 amount SARS-CoV-2 (D'Aoust et al., 2021; Graham et al., 2021; Westhaus et al.,  
288 2021).



289

290 **Fig. 1.** Percent recovery and statistical analysis for each method.

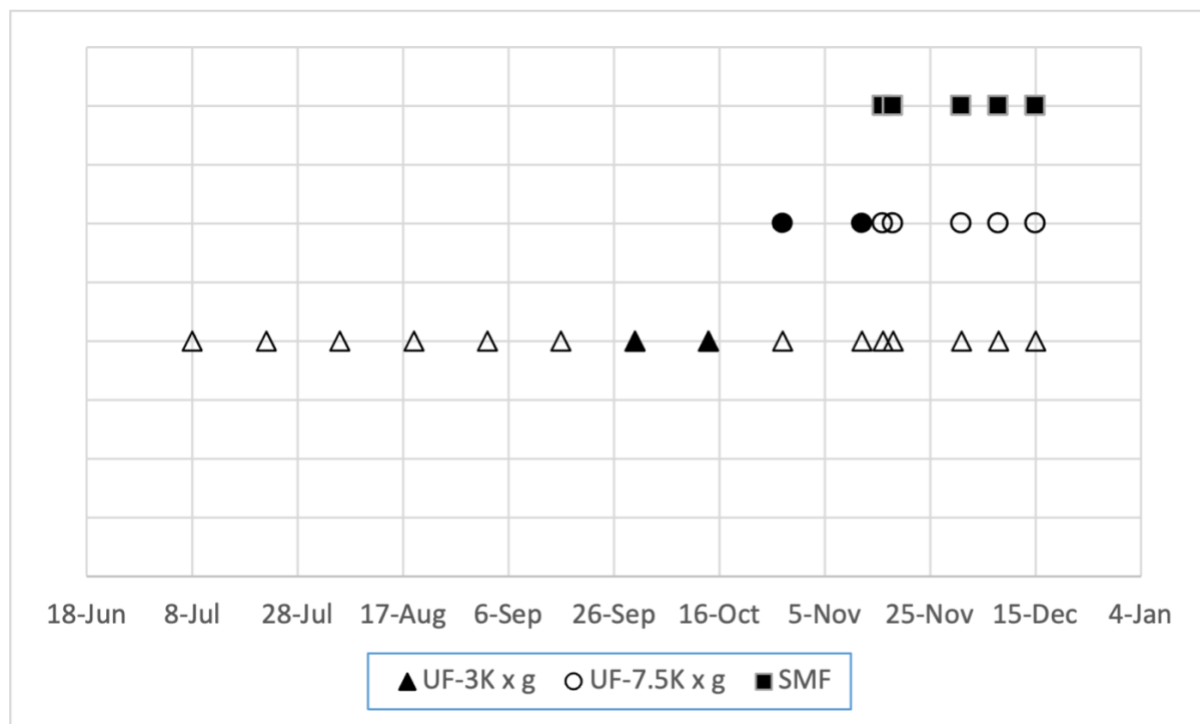
291 SMF was later employed to concentrate and detect SARS-CoV-2 in wastewater  
292 samples. Using Armored RNA as a control, 15.27%  $\pm$  3.32% of recovery was  
293 achieved from the spiked wastewater samples (Fig. 1.). SMF has the highest  
294 recovery efficiency with the smallest standard deviation whereas UF-7.5K x g has the  
295 lowest recovery efficiency with 5 negative samples out of 6 samples. This method did  
296 not employ a prefiltration step with cheesecloth and low-protein binding 0.45 and 0.2  
297  $\mu\text{m}$  47-mm membrane filters. Therefore, the losses due to the elimination of solid  
298 particles were minimized and might have been reflected through the higher  
299 percentage and lower variation in recovery. Percent recovery values for SMF were  
300 comparable to the recovery values reported by Philo et al. (2021). They also reported  
301 30% positivity rate for SARS-CoV-2 with SMF.

302 3.2. *Detection of SARS-CoV-2 in influent and effluent wastewater and primary*  
303 *sludge*

304 3.2.1. Virus concentration method determines the detection of SARS-CoV-2 in  
305 influent samples.

306 Table 3 shows concentrations of SARS-CoV-2 in wastewater and sludge samples  
307 collected during the sampling period. Three different concentration methods, namely  
308 UF-3K x g, UF-7.5K x g and SMF, were applied (Fig. 2). UF-3K x g and UF-7.5K x g  
309 methods required a prefiltration step with 0.45 and 0.2  $\mu\text{m}$  filters to eliminate the  
310 effects of solids on ultrafiltration performance and separate viral fraction from  
311 bacterial fraction. On the other hand, SMF did not require any prefiltration step, and  
312 therefore SARS-CoV-2 particles on solids were also concentrated with this method.  
313 All influent and effluent samples were processed using UF-3K x g method (Fig. 2).  
314 Influent samples collected between October 28<sup>th</sup> and December 15<sup>th</sup> were processed  
315 with both UF-3K x g AND UF-7.5K x g methods. They were first concentrated with

316 UF-7.5K x g method, and the negative samples were further processed with UF-3K x  
317 g method within 4 days of sampling. As samples were negative when processed with  
318 UF-3K x g and UF-7.5K x g methods between November 16<sup>th</sup> and December 15<sup>th</sup>  
319 (Fig. 2), SMF method was applied delayed (Table 1) to concentrate SARS-CoV-2  
320 from these samples stored at 4 °C. SARS-CoV-2 was detected in all influent samples  
321 collected between September 30<sup>th</sup> and December 15<sup>th</sup>, except October on 28<sup>th</sup>.  
322 SARS-CoV-2 was detected only in influent samples collected from SESTP on  
323 October 28<sup>th</sup>.



324  
325 **Fig. 2.** Detection of SARS-CoV-2 RNA in influent samples with different  
326 concentration methods. Filled shapes represent the samples that are SARS-CoV-2  
327 positive, i.e.  $C_T$  is <40.  
328 Non-detection of SARS-CoV-2 with UF-3K x g and UF-7.5K x g methods can be  
329 attributed to several factors, such as degradation during transportation and storage of  
330 samples (Ahmed et al., 2020b; Bivins et al., 2020a; Hokajärvi et al., 2021a; Hokajärvi

331 et al., 2021b), losses during virus concentration (Chik et al., 2021; Ye et al., 2016),  
332 losses during extraction, and PCR related issues, such as inhibition and incomplete  
333 reverse transcription (Bustin et al., 2009). Since the variables in this study were the  
334 storage period at 4°C and virus concentration methods, the first two factors could  
335 explain the variations in detection with different concentration methods. SARS-CoV-2  
336 was detected with UF-3K x g method only on September 30<sup>th</sup> and October 14<sup>th</sup> (Fig.  
337 2). All samples processed 4 days after collection were negative, possibly due to  
338 decay of SARS-CoV-2 at 4°C (Ahmed et al., 2020b; Hokajärvi et al., 2021a) and  
339 partitioning of SARS-CoV-2 to the solid phase rather than liquid phase (Chik et al.,  
340 2021). The time required for the decay of 90% ( $T_{90}$ ) of N1 and N2 genes at 4°C was  
341 reported as  $27.8 \pm 4.45$  and 36 days by Ahmed et al. (2020b) and Hokajärvi et al.  
342 (2021a). Considering that  $T_{90}$  values being much greater than four days, the decay of  
343 SARS-CoV-2 might not have lowered SARS-CoV-2 concentration in influent samples  
344 to undetectable levels. Moreover, Markt et al. (2021) reported a minimal reduction in  
345 SARS-CoV-2 concentrations in 9 days when stored at 4°C. Therefore, attachment of  
346 SARS-CoV-2 to solids, concentration method, and variation in recovery efficiency are  
347 plausible causes for the non-detection of SARS-CoV-2. Several studies have  
348 reported a higher affinity of enveloped viruses (mouse hepatitis virus [MHV] and  
349 *Pseudomonas* phage  $\Phi 6$ ) to attach solid particles in wastewater compared to non-  
350 enveloped viruses (Ye et al., 2016), which might be the case for the non-detection of  
351 SARS-CoV-2 in influent filtrates in this study. Attachment of SARS-CoV-2 to solids  
352 and variations in recovery efficiencies together possibly resulted in non-detection.  
353 This was further confirmed by the analysis of solid particles retained on the filters.  
354 SARS-CoV-2 was detected in all solids retained on the filters except for the sample  
355 collected from WESTP on October 14<sup>th</sup> (Table 4). The difference of one order of



356 magnitude between SARS-CoV-2 concentrations in solids and filtrate indicated the  
357 significance of solid phase partitioning of SARS-CoV-2. For some samples, SARS-  
358 CoV-2 concentration was even higher in solids. Hokajärvi et al. (2021a) also reported  
359 a higher detection frequency of SARS-CoV-2 N2 gene frequency in solids (89%)  
360 compared to that in the supernatant (67%). In most cases, the virus might  
361 predominate in solid phase (Chik et al., 2021). Similarly, some other studies also  
362 emphasized solids-associated behavior of SARS-CoV-2 by taking the absorption of  
363 viral particles to solids into consideration and reporting the correlations between virus  
364 concentration and case data (D'Aoust et al., 2021; Graham et al., 2021; Peccia et al.,  
365 2020). Effects of freezing and thawing on SARS-CoV-2 concentrations in solids  
366 should also be considered in this study. We extracted from solids on filters stored at -  
367 20°C that were later subjected to freeze-thaw once. Markt et al. (2021) reported a  
368 significant SARS-CoV-2 reduction in influent samples subjected to one freeze-thaw  
369 cycle. In comparison with these results, Simpson et al. (2021) and Hokajärvi et al.  
370 (2021a) observed a relatively lower reduction of SARS-CoV-2 in solids after one  
371 cycle of freeze-thaw, but still up to 60% of reduction. Considering current literature,  
372 the actual SARS-CoV-2 concentrations in solids might be higher than the measured  
373 concentrations. Moreover, the presence of solids in wastewater might enhance the  
374 stability of SARS-CoV-2 (Kitajima et al., 2020).

375 Samples processed with UF-7.5K x g exhibited similar behavior to samples  
376 processed with UF-3K x g. SARS-CoV-2 was detected with this method only on  
377 October 28<sup>th</sup> and November 12<sup>th</sup> (Fig. 2 and Table 3) in influent filtrates. As discussed  
378 for UF-3K x g, retention of solids during prefiltration with 0.45 and 0.2 µm filters might  
379 result in the non-detection of SARS-CoV-2 in influent samples. In addition to the  
380 elimination of solids particles, increasing the centrifugation speed to 7500 x g might

381 have led to the passage of viruses through the filter and/or binding of viruses onto  
382 filters. Indeed, the inability of recovery tests for virus concentration methods in  
383 determining the true recovery efficiencies can cause biases in the detection and  
384 quantitation of viruses in wastewater samples. Since SARS-CoV-2 is predominantly  
385 in contact with fecal matter in the wastewater matrix during the transportation to the  
386 WWTPs via sewer systems, recovery efficiency determination approaches, which  
387 are generally based on a spike-and-recovery approach, might not sufficiently reflect  
388 the actual recovery values of SARS-CoV-2 (Chik et al., 2021). This could be due to  
389 several reasons in the current study. First, there were only 30 minutes between  
390 sample spiking and processing in this study. Secondly, physicochemical  
391 characteristics of the spiked wastewater samples could be significantly different from  
392 influent samples that were processed in this study. Amoah et al. (2022) previously  
393 demonstrated the effects of pH, ammonia, and total solids on viral detection and  
394 SARS-CoV-2 concentration. Thus, the actual recovery of SARS-CoV-2 might be  
395 much lower than the assessed recovery efficiencies for UF-3K x g and UF-7.5K x g  
396 considering spike-and-recovery approaches and variations in physicochemical  
397 characteristics of the samples. Furthermore, higher concentrations of SARS-CoV-2  
398 were observed in solids (Table 4) when total solids concentrations were higher in the  
399 samples collected from NESTP between October 28<sup>th</sup> and November 18<sup>th</sup> (Table S4).  
400 This increase can be attributed to the increase in total solids due to the partitioning of  
401 SARS-CoV-2 to solid phase (Chik et al., 2021). The relationship between case data  
402 (Fig. 3) and SARS-CoV-2 concentration in solids during this period should not be  
403 overlooked, as discussed in section 3.2.4.

404 **Table 3.** Concentration of SARS-CoV-2 RNA in influents of three WWTPs. Influent samples collected between November 16<sup>th</sup> and December 15<sup>th</sup> (shown in a box) were  
 405 late processed samples with SMF

Sampling Date	NESTP						SESTP						WESTP					
	Influent (GC/L)		Primary Sludge (GC/mL)		Effluent (GC/L)		Influent (GC/L)		Primary Sludge (GC/mL)		Effluent (GC/L)		Influent (GC/L)		Primary Sludge (GC/mL)		Effluent (GC/L)	
	N1	N2	N1	N2	N1	N2	N1	N2	N1	N2	N1	N2	N1	N2	N1	N2	N1	N2
8-Jul	0	0	-	-	0	0	0	0	-	-	0	0	0	0	-	-	0	0
22-Jul	0	0	-	-	0	0	0	0	-	-	0	0	0	0	-	-	0	0
5-Aug	0	0	-	-	0	0	0	0	-	-	0	0	0	0	-	-	0	0
19-Aug	0	0	-	-	0	0	0	0	-	-	0	0	0	0	-	-	0	0
2-Sep	0	0	-	-	0	0	0	0	-	-	0	0	0	0	-	-	0	0
16-Sep	0	0	-	-	0	0	0	0	-	-	0	0	0	0	-	-	0	0
30-Sep	6,087	25,713	-	-	0	0	8,778	20,009	-	-	0	0	25,087	47,557	-	-	0	0
14-Oct	13,222	34,751	-	-	0	0	26,670	47,714	-	-	0	0	28,894	47,226	-	-	0	0
28-Oct	0	0	-	-	0	0	7,544	21,084	-	-	0	0	0	0	-	-	0	0
12-Nov	3.3E+6	2.5E+6	7,980	4,960	-	-	1.2E+6	3.4E+6	3,140	2,740	-	-	9.6E+5	1.1E+6	2,080	660	-	-
16-Nov	51,400	26,668	96,200	8,860	-	-	12,964	17,410	2,400	1,360	-	-	16,506	4,372	0	0	-	-
18-Nov	16,249	55,512	8,540	6,480	-	-	5,843	17,412	3,280	3,040	-	-	13,762	11,844	0	380	-	-
1-Dec	20,980	16,833	7,480	6,740	-	-	11,261	6,780	3,100	2,260	-	-	5,519	2,214	0	260	-	-
8-Dec	15,722	11,463	12,580	5,860	-	-	4,984	9,685	7,560	2,760	-	-	9,007	5,300	820	180	-	-
15-Dec	20,371	13,120	3,220	1,400	-	-	17,209	8,188	3,020	740	-	-	5,535	5,211	5,660	2,600	-	-

406

SARS-CoV-2 was not detected between November 16<sup>th</sup> and December 15<sup>th</sup> when samples were processed with UF-3K x g and UF-7.5K x g methods. However, SARS-CoV-2 was detected in these samples using SMF (Fig. 2 and Table 3), although the sample processing was delayed between 46 and 75 days (Fig. 2). The successful detection of the virus was most probably because of the inclusion of both solids and supernatant into sample processing with SMF. The positive results confirmed that SARS-CoV-2 might predominate in solid phase and have higher stability in wastewater when attached to solids. An inter-laboratory study processing wastewater samples collected on the same day from a WWTP in Winnipeg also reported that SARS-CoV-2 was detected only by the laboratories processing samples with the methods focusing on solids (Chik et al., 2021). Another study on the partition of enveloped viruses to wastewater solids strengthens the claim of such solid-associated behavior with concentrations of enveloped viruses in solids found 1000 times higher than those in influent on a per mass basis (Ye et al., 2016). As a matter of fact, many other studies have suggested that a wastewater solids-based measurement of SARS-CoV-2 might be a more sensitive approach than a wastewater supernatant-based one (D'Aoust et al., 2021; Graham et al., 2021; Peccia et al., 2020; Westhaus et al., 2021). Moreover, input volumes of SMF (500 mL), UF-3K x g (120 mL) and UF-7.5K x g (120 mL) might be another factor determining detection of SARS-CoV-2, especially when the virus is not abundant in the samples.

**Table 3.** SARS-CoV-2 RNA concentration in influent solids from NESTP, SESTP and WESTP.

Date	NESTP		SESTP		WESTP	
	N1 (GC/L)	N2 (GC/L)	N1 (GC/L)	N2 (GC/L)	N1 (GC/L)	N2 (GC/L)
2-Sep	0	0	0	0	0	0
16-Sep	0	0	0	0	0	0
30-Sep	-	-	232,059	367,283	75,185	0
14-Oct	75,422	0	76,814	0	0	0
12-Nov	335,397	516,635	149,704	95,908	49,617	78,529
16-Nov	302,821	113,570	0	26,192	159,752	29,619
18-Nov	626,217	242,533	128,595	42,033	307,246	147,921
1-Dec	43,106	26,877	69,835	49,772	120,428	60,634
8-Dec	45,194	21,513	31,191	14,206	15,026	12,649
15-Dec	-	-	-	-	-	-

SARS-CoV-2 can be detectable in both influent wastewater and solids long after storage at 4°C (Ahmed et al., 2020b; Hokajärvi et al., 2021a; Markt et al., 2021). The time required for 90 % reduction of SARS-CoV-2 in influent wastewater at 4°C was reported to be between 28, 36, and 52 days for the genomic targets, N1, N2 and E, respectively (Ahmed et al., 2020b; Hokajärvi et al., 2021a). On the other hand, only a one order of magnitude reduction of SARS-CoV-2 in solids was observed for the samples stored at 4°C over 100 days (Markt et al., 2021). SARS-CoV-2 was detected at higher frequencies and concentrations in solids compared to those in wastewater supernatant at the end of a period of 84 days (Hokajärvi et al., 2021a). Although the studies on the stability and detection of SARS-CoV-2 in influent and solids are

limited, the current findings point out the predominant partition of SARS-CoV-2 to solid phase and higher stability of SARS-CoV-2 in solids. The results of this study, together with previous studies (Chik et al., 2021; Hokajärvi et al., 2021a; Markt et al., 2021), underscores the importance of the inclusion of both solids and supernatant fractions in wastewater processing for the detection of SARS-CoV-2. However, adsorption capacity of SARS-CoV-2 to wastewater solids needs to be investigated.

### 3.2.2. Detection in primary sludge samples

Both N1 and N2 genomic targets of SARS-CoV-2 were detected in all primary sludge samples collected from NESTP and SESTP while they were not detected on November 16<sup>th</sup>, and only N2 was detected on November 18<sup>th</sup> and December 1<sup>st</sup> in the samples collected from WESTP (Table 3). The input volume of primary sludge samples processed for the detection of SARS-CoV-2 in this study was only 300  $\mu$ L, which is much lower than the input volumes in previous studies (Graham et al., 2021; Peccia et al., 2020). Still SARS-CoV-2 was detected, indicating the high density of SARS-CoV-2 in primary sludge.

Detection of SARS-CoV-2 in primary sludge samples could be associated with the input volume and total solids in the samples. Low input volumes can cause biases in the detection and quantification of SARS-CoV-2 when virus concentration in the sample is low, and the samples are not homogenous in terms of total solids and SARS-CoV-2 distribution. Considering the high affinity of enveloped viruses to attach to the solids particles (Ye et al., 2016), total solids concentration can be another determinant of detection and quantification of SARS-CoV-2 in primary solids in addition to the community infection dynamics. In fact, concentration of SARS-CoV-2 was generally the highest in the samples collected from NESTP with an average

primary sludge density of  $3.53 \pm 0.84$  % and was generally the lowest in the samples collected from WESTP with an average sludge density of  $0.37 \pm 0.06$  % (Table S5). This statement assumes homogeneous distribution of prevalence and incidence throughout the city of Winnipeg on the sampling days based on the high correlation between influent viral concentrations in WWTPs ( $r > 0.91$  for N1 and  $r > 0.72$  for N2) (Table S6). Higher input volumes should be considered for consistent and sensitive detection and quantification of the viral RNA in sludge samples.

**Table 4.** SARS-CoV-2 RNA concentration in influent solids from NESTP, SESTP and WESTP.

Date	NESTP		SESTP		WESTP	
	N1 (GC/L)	N2 (GC/L)	N1 (GC/L)	N2 (GC/L)	N1 (GC/L)	N2 (GC/L)
2-Sep	0	0	0	0	0	0
16-Sep	0	0	0	0	0	0
30-Sep	-	-	232,059	367,283	75,185	0
14-Oct	75,422	0	76,814	0	0	0
12-Nov	335,397	516,635	149,704	95,908	49,617	78,529
16-Nov	302,821	113,570	0	26,192	159,752	29,619
18-Nov	626,217	242,533	128,595	42,033	307,246	147,921
1-Dec	43,106	26,877	69,835	49,772	120,428	60,634
8-Dec	45,194	21,513	31,191	14,206	15,026	12,649
15-Dec	-	-	-	-	-	-

### 3.2.3. Detection in effluent samples

SARS-CoV-2 was not detected in both secondary and final effluent samples of all three WWTPs (Table 3), although it is worth mentioning that WESTP employs solar disinfection, which effectively reduces bacteria and is questionable in removing viruses, especially in cold climate conditions (Parsa et al., 2021). Employing UV disinfection, NESTP and SESTP might have effectively reduced SARS-CoV-2 concentration below detectable levels in final effluent. SARS-CoV-2, being an enveloped virus, is expected to be more sensitive to disinfection processes (UV, ozonation, and chlorination) than non-enveloped viruses (Chen et al., 2021; Saawarn and Hait, 2021). Non-detection of SARS-CoV-2 in tertiary-treated effluent samples was also reported elsewhere (Randazzo et al., 2020; Sherchan et al., 2020), indicating the efficacy of disinfection processes in the removal of SARS-CoV-2 considering high positivity rates (>83 %) in influent samples. This claim was further supported by the occurrence of SARS-CoV-2 in secondary-treated effluent (before disinfection) samples (Haramoto et al., 2020; Randazzo et al., 2020).

SARS-CoV-2 is removed not only by disinfection processes but also primary and secondary treatment processes, which can also effectively reduce SARS-CoV-2 concentration in the WWTPs (Balboa et al., 2020; Randazzo et al., 2020; Sherchan et al., 2020). Detection of SARS-CoV-2 in very low volumes of primary sludge samples in this study might indicate a significant removal of SARS-CoV-2 with primary treatment. While removal of SARS-CoV-2 with primary, secondary and tertiary treatments could explain non-detection of SARS-CoV-2 in effluent samples to a great extent, elimination of solid particles with prefiltration of effluent samples with 0.45 and 0.2  $\mu\text{m}$  filters could be another factor considering the attachment of SARS-CoV-2 to solids. However, more studies are needed to fully uncover the fate of



SARS-CoV-2 in WWTPs and the effects of virus concentration methods and input volume on the detection and quantification of SARS-CoV-2 in effluent samples.

#### 3.2.4. Detection of SARS-CoV-2 relates to the number of cases and test positivity rate

SARS-CoV-2 was first detected at a concentration of <50 gene copies per liter (GC/mL) on September 30<sup>th</sup> in all influent wastewater samples collected from NESTP, SESTP, and WESTP (Table 3) when the number of the reported new cases and active cases in Winnipeg were 25 and 321, respectively (Fig. 3). This first detection concentration on September 30<sup>th</sup> went up to 400 GC/mL after the concentration of the viral RNA in the solids was added to the concentration in supernatant. Detection of SARS-CoV-2 in wastewater samples collected from a WWTP in Winnipeg on August 31<sup>st</sup> was first reported by Chik et al. (2021) at trace concentrations (<20 GC/mL), with the concentration methods focusing on solid fraction when number of the reported new and active cases were 11 and 85, respectively. Both results suggest a larger number of new and active cases consisting of asymptomatic, presymptomatic, and recovering cases of COVID-19 in the community. This is consistent with the estimations of the actual number of infections being 3 to 20 (Wu et al., 2020) and 6 to 24 times (Havers et al., 2020) higher than reported cases in the U.S. A study by Hong et al. (2021) focusing on the estimation of the minimum number of SARS-CoV-2 infected cases for the detection of viral RNA in wastewater estimated a minimum number of active cases of 253 to 459 positive cases per 10,000 population to detect SARS-CoV-2 in wastewater, which is much higher than the number of active cases on the day of the first detection in Winnipeg considering the population of Winnipeg (766,900) (Winnipeg, 2021). However, the reported range of active cases needed for the detection of SARS-CoV-

2 might be a system- or site-specific estimation since the detection of SARS-CoV-2 in wastewater depends on many factors, including sampling frequencies, concentration methods, and their recovery efficiencies, RT-qPCR detection performance, sample size, daily wastewater flow rates (dilution factor), and environmental factors which can affect the persistence and abundance of SARS-CoV-2 in wastewater (Hong et al., 2021). Moreover, new cases predominantly contribute to the concentration of SARS-CoV-2 in wastewater rather than active cases (Gerrity et al., 2021; Wu et al., 2022) due to higher viral shedding rates in the very early stages of the infection (Benefield et al., 2020; He et al., 2020; Wei et al., 2020; Wölfel et al., 2020). Therefore, the number of active cases, without the data regarding new and early-stage cases, may not be enough in determining the minimum number of cases to detect SARS-CoV-2 in wastewater.

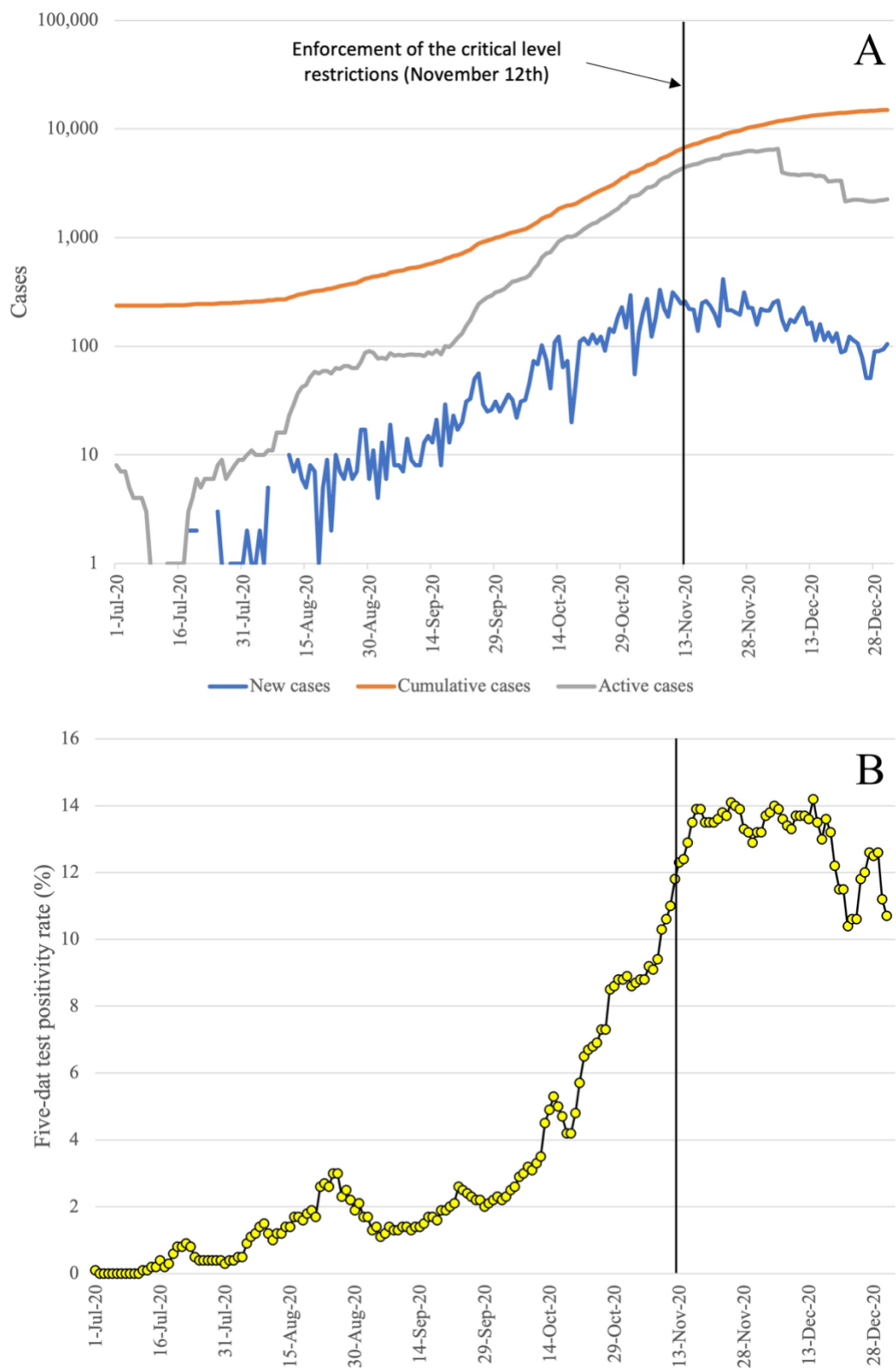


**Fig. 3.** COVID-19 infection dynamics in Winnipeg. A) Temporal changes in the numbers of new, active, and cumulative cases during sampling period. B) Five-day test positivity rates during the sampling period.

The difference between symptom onset and test confirmation suggests that time-lag might be another explanation for the detection of SARS-CoV-2 when the number of active cases was low. There is also a typical 4 to 5 day incubation period before onset of the symptoms (He et al., 2020; Li et al., 2020). A possible effect of time-lag can be further confirmed by the sharp increase in the number of cases and five-day test positivity rate (Fig. 3) after September 30<sup>th</sup>. Between the first sampling date, July 8<sup>th</sup>, and September 30<sup>th</sup>, the five-day test positivity rate fluctuated between 0.0% and 3.0 % (Fig. 3) (Manitoba, 2021). On September 30<sup>th</sup>, the test positivity rate was 2.1 %, and henceforth a constant increase in the test positivity rate until mid-December was noticed, with a peak test positivity rate of 14.2 % on December 14<sup>th</sup>. During this period, we detected SARS-CoV-2 in all influent samples (including solids fractions) collected from three wastewater treatment plants, except on October 28<sup>th</sup> (Table 3), using different concentration methods.

Previous studies have reported associations between the concentration of SARS-CoV-2 in primary settled solids and COVID-19 cases (Graham et al., 2021; Peccia et al., 2020). In this study, SARS-CoV-2 was detected in almost all primary sludge samples. In the previous sections, the fluctuations in the concentration of SARS-CoV-2 were partly associated with total solids in the samples. A direct correlation between concentrations and reported cases is intentionally avoided due to low-resolution sample collection and small input volumes of primary sludge. These two factors cause some difficulties in justifying the fluctuations in SARS-CoV-2 concentrations in primary sludge samples. In other words, it is not clear if solids, the number of infections, or a combination of them cause fluctuations in SARS-CoV-2 concentrations. High-resolution sample collection (at least weekly) and larger input

volumes could generate more reliable and consistent results for a wastewater surveillance study.

### 3.3. Estimation of Concentrations and Shedding Cases

Using reported decay rates for N1 and N2 gene fragments (Ahmed et al., 2020b; Hokajärvi et al., 2021a), initial concentrations of SARS-CoV-2 in the late processed influent samples, collected between November 16<sup>th</sup> and December 15<sup>th</sup>, were estimated and then converted into normalized concentration using eqn. 1. Reported COVID-19 infection dynamics and observed (measured and back-trajectory modeled) concentrations were compared with infection dynamics and generated by model 2 as an attempt to justify models and understand the course of COVID-19 infection dynamics in the city. Lack of information regarding population and COVID-19 infection dynamics in each sewershed is one of the limitations of this study, preventing us from doing a sewershed-based analysis.

Peak concentrations of SARS-CoV-2 were observed on the day when critical-level restrictions were enforced and the following 4<sup>th</sup> and 6<sup>th</sup> day (Fig. 4). Other observed concentrations after the first detection were generally in close proximity with the modeled concentrations for at least one genomic target. Different decay rates for N1 and N2 resulted in higher concentrations of N1 for back-trajectory modeled samples collected between November 16<sup>th</sup> and December 15<sup>th</sup>, while the difference between N1 and N2 concentrations for the rest of the samples was smaller than 0.35 on log<sub>10</sub> scale (Fig. 4). The decay rate of N1 was calculated based on the degradation of genomic signals of gamma-irradiated SARS-CoV-2 by Ahmed et al. (2020b) and had a higher standard deviation of 15% and lower R<sup>2</sup> of 0.79 compared to those values of N2, which were based on degradation of active SARS-CoV-2 (Hokajärvi et al., 2021a) (Table 2). Gamma irradiation of SARS-CoV-2 and relatively higher variations

in the decay rate of N1 might result in significant biases in such a back-trajectory modeling approach. Therefore, we mostly consider N2 concentrations for back-trajectory modeled samples in the discussion.

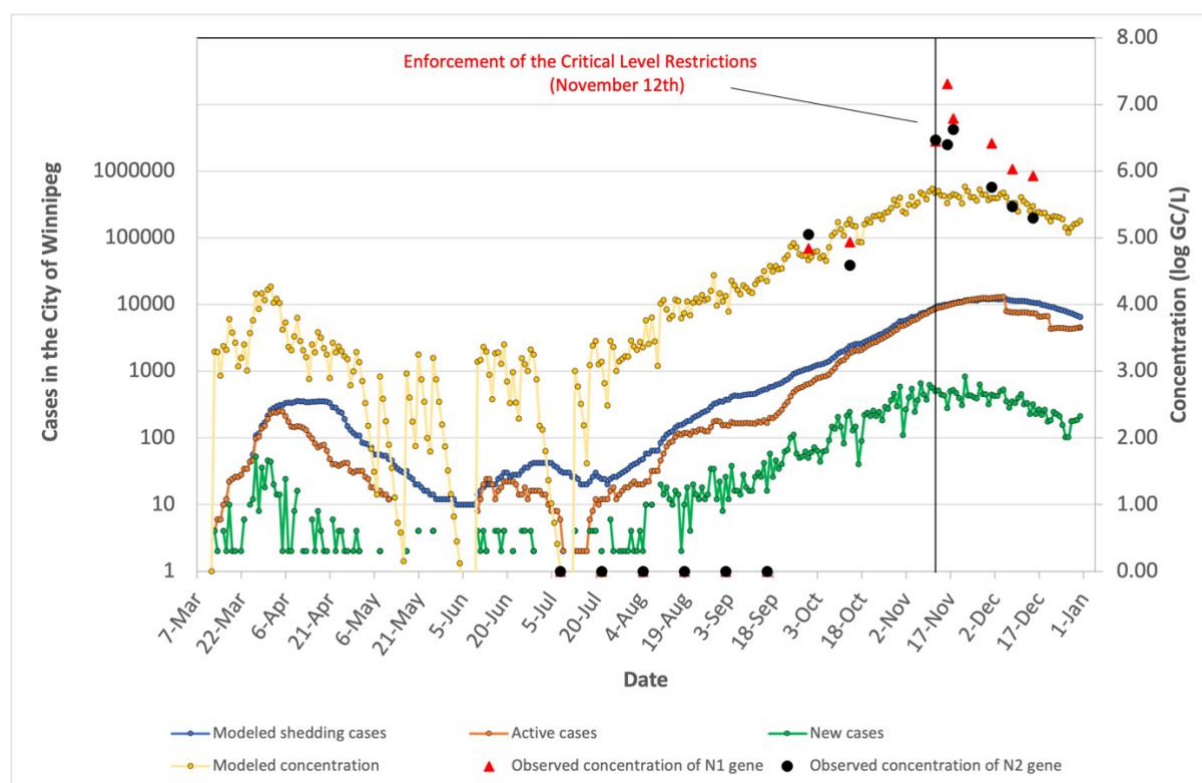


**Fig. 4.** Modeled (yellow circles) and observed concentrations (red triangles and black circles) of SARS-CoV-2 RNA as log<sub>10</sub> concentrations and COVID-19 infection dynamics from the beginning of the outbreak in Winnipeg. Observed concentrations between September 30<sup>th</sup> and November 12<sup>th</sup> are the sum of the concentration in solids and filtrates since the latter concentrations were obtained using SMF which concentrates viruses from both supernatant and solids. Observed concentrations between November 16<sup>th</sup> and December 15<sup>th</sup> are estimated using eqn. 3. Observed concentrations are represented for both N1 (red triangles) and N2 (black circles). Green circles represent new cases in Winnipeg corrected with an ascertainment ratio of 2. Oranges circles represent active cases in Winnipeg corrected with an

ascertainment ratio of 2. Blue circles represent modeled shedding cases in Winnipeg, i.e. modeled active cases.

The critical level restrictions in Manitoba were applied when extensive community transmission of COVID-19 occurred, outbreaks could not be controlled, and a heavy toll on the health-care system is expected. With the enforcement of the restrictions on November 12<sup>th</sup>, gatherings and travels were extremely restricted, and schools and non-essential businesses were closed. Bearing in mind that the outbreak and transmission are at the critical levels when the restrictions are applied, the occurrence of a much higher number of new cases compared to reported numbers is most likely because of the limited testing capacity at the peak times and time-lag between the incubation period of SARS-CoV-2, onset of the symptoms and test confirmation (He et al., 2020; Li et al., 2020). In this study, such a scenario was validated with the observed concentrations of SARS-CoV-2 in influent that peaked following the enforcement in November and significantly lowered to the modeled concentrations in December as the outbreak was contained. The difference between the observed concentrations of N2 and modeled concentrations (0.79 to 0.97 on log<sub>10</sub> basis) in November suggests that the actual number of cases might be much higher than reported numbers, which is further supported by the sharp increase in test-positivity rates and the number of new cases (Fig. 3). These findings correspond to the findings of Havers et al. (2020), reporting that the actual number of cases can be as high as 24 times of reported numbers.

In general, observed concentrations were sensitive to the fluctuations in test-positivity rates and the number of new cases except for the samples collected in November. Model 2 assumed an ascertainment ratio of 2, which is an optimistic assumption considering ascertainment ratios up to 24 in the literature (Havers et al., 2020; Wu et

al., 2020). While an ascertainment ratio of 2 in the model generated comparable concentrations with the observed concentrations for September, October, and December samples, a higher ascertainment ratio might come into question during the peak times in November. The high concentrations and ascertainment ratios in November can be explained by the high transmission rates of the disease and the number of asymptomatic and presymptomatic cases around this period. After the enforcement of critical level restrictions, public mobility and disease transmission were expected to be minimized. However, the number of new cases and the test-positivity rate remained high during the sampling in November and December, most likely due to time-lag associated with the peaking of viral load and disease transmissivity prior to symptom onset (Benefield et al., 2020; He et al., 2020; Wei et al., 2020). Probably most individuals were infected around the first day of the enforcement but developed symptoms later, which was in agreement with the typical incubation period of 4-5 days before symptom onset (Guan et al., 2020; Lauer et al., 2020; Li et al., 2020), and only sought healthcare and underwent testing after symptom onset. SARS-CoV-2 load in December might be due to prolonged shedding from individuals infected earlier. Additionally, individuals infected before the enforcement can infect other people living with them in subsequent days, and disease transmission can still be high among essential workers and their families after the enforcement.

Estimation of SARS-CoV-2 concentration based on shedding rate and reported cases has been previously studied with an emphasis on the significant contribution of newly infected individuals to SARS-CoV-2 loads in wastewater and occurrence of the highest fecal shedding rates in the first days of infection before symptoms develops and tests are conducted (Gerrity et al., 2021; Wu et al., 2022). They also reported



high similarity between the observed and modeled concentrations, which validates the efficacy of such models to estimate concentration and infection dynamics.

Sensitivity of SARS-CoV-2 levels in wastewater to the fluctuations in the number of new cases and test-positivity rates in this study suggest that an initial burst of viral shedding may occur in the very early stages of COVID-19 infection even before symptom onset and may be followed by a prolonged period of lower shedding rates up to 30 days as reported by Chen et al. (2020), Hoffmann and Alsing (2021), Wölfel et al. (2020) and (Wu et al., 2022).

Our data suggest that a back-trajectory model as a function of decay rate and time may be used to estimate initial concentrations of late processed samples as it fit the modeled concentrations and fluctuations in new cases. High-resolution sampling and site-specific decay rates may help to validate and improve the model. Time-lag, testing capacity, and test-positivity rates in addition to the reported cases and shedding rate should also be considered for the shedding rate-based models to obtain better model fits and estimations.

#### 4. Conclusions

Wastewater surveillance of COVID-19 has been considered an early-warning tool for potential outbreaks and an informative method to characterize COVID-19 infection dynamics. However, researchers have not reached a consensus on sample collection and processing, and data analysis. Furthermore, the potential discharge of SARS-CoV-2 from wastewater treatment plants to the environment is another issue that requires a comprehensive investigation of the fate of SARS-CoV-2 throughout the wastewater treatment process.

The current study focused on the detection of SARS-CoV-2 in wastewater and sludge samples and the relationship between detection and infection dynamics in Winnipeg. Our results showed that SARS-CoV-2 might predominate in solids. Concentration methods focusing on supernatant and solids fractions may perform better in virus recovery, especially for enveloped viruses. Thus, the type of concentration method may significantly affect SARS-CoV-2 recovery from influent samples.

SARS-CoV-2 might be substantially removed during primary and secondary treatment as SARS-CoV-2 was detected in influent and primary sludge but not in secondary and final effluents. The high affinity of SARS-CoV-2 to solids and detection of SARS-CoV-2 in primary sludge samples at high concentrations suggest sludge line as a potential removal mechanism and a sampling spot for wastewater surveillance. Improvement in processing sludge samples for viral concentration and detection is required to gain more insight into the fate of SARS-CoV-2 in sludge line and optimize sampling and processing.

In addition to the detection and fate of SARS-CoV-2 in WWTPs, the proposed study underlines the relationship between SARS-CoV-2 levels in influent samples and infection dynamics characterized by increasing COVID-19 incidence and prevalence during the sampling period. Both observed and modeled concentrations were sensitive to the fluctuations in new cases and test-positivity rates, suggesting an early burst of viral shedding in infected individuals. During the peak times, the number of infections can be much higher than the number of reported cases considering the time-lag between infection and test confirmation, and asymptomatic infections. To confirm our findings and improve such shedding rate-based models, additional studies with higher sampling resolution and the models informed by some other factors factors, such as time-lag, test capacity, and test-positivity rates, are required.

Overall, this study demonstrates that SARS-CoV-2 may predominate in solids, and wastewater surveillance of COVID-19 can provide valuable insights into infection dynamics prior to clinical test confirmations.

## **Acknowledgments**

We thank the City of Winnipeg, the management, and operators at the NESTP, SESTP, and WESTP for collecting samples and providing information regarding wastewater characteristics, in particular Jong Hwang, Brendan Hellrung, Mark Lefko, Jorge Martins, and Shaun Walker. We acknowledge Ms. Shana Mann and Miss Jocelyn Zambrano (University of Manitoba) for nucleic acid extraction from solids. We also thank Tri Le (University of Manitoba) for proofreading.

**Funding:** This work was supported by NSERC Alliance Covid-19 Grant (Grant No. 431401363, 2020-2021).

## **CRedit authorship contribution statement**

**Kadir Yanaç:** Conceptualization, Methodology, Validation, Formal Analysis, Investigation, Data Curation, Visualization, Writing & Original Draft, . **Adeola**

**Adegoke:** Software, Formal Analysis. **Liqun Wang:** Software, Formal Analysis.

**Qiuyan Yuan:** Conceptualization, Methodology, Validation, Resources, Review & Editing, Supervision, Project Administration, Funding Acquisition. **Miguel Uyaguari:**

Conceptualization, Methodology, Validation, Resources, Review & Editing, Supervision, Project Administration, Funding Acquisition.

## **Declaration of competing interest**

The authors declare no conflicts of interest.

## References

- Ahmed, W., Angel, N., Edson, J., Bibby, K., Bivins, A., O'Brien, J.W., Choi, P.M., Kitajima, M., Simpson, S.L., Li, J., Tschärke, B., Verhagen, R., Smith, W.J.M., Zaugg, J., Dierens, L., Hugenholz, P., Thomas, K.V. and Mueller, J.F. 2020a. First confirmed detection of SARS-CoV-2 in untreated wastewater in Australia: A proof of concept for the wastewater surveillance of COVID-19 in the community. *Science of The Total Environment* 728, 138764.
- Ahmed, W., Bertsch, P.M., Bibby, K., Haramoto, E., Hewitt, J., Huygens, F., Gyawali, P., Korajkic, A., Riddell, S., Sherchan, S.P., Simpson, S.L., Sirikanchana, K., Symonds, E.M., Verhagen, R., Vasan, S.S., Kitajima, M. and Bivins, A. 2020b. Decay of SARS-CoV-2 and surrogate murine hepatitis virus RNA in untreated wastewater to inform application in wastewater-based epidemiology. *Environmental Research* 191, 110092.
- Ahmed, W., Bertsch, P.M., Bivins, A., Bibby, K., Farkas, K., Gathercole, A., Haramoto, E., Gyawali, P., Korajkic, A., McMinn, B.R., Mueller, J.F., Simpson, S.L., Smith, W.J.M., Symonds, E.M., Thomas, K.V., Verhagen, R. and Kitajima, M. 2020c. Comparison of virus concentration methods for the RT-qPCR-based recovery of murine hepatitis virus, a surrogate for SARS-CoV-2 from untreated wastewater. *Science of The Total Environment* 739, 139960.
- Alygizakis, N., Markou, A.N., Rousis, N.I., Galani, A., Avgeris, M., Adamopoulos, P.G., Scorilas, A., Lianidou, E.S., Paraskevis, D., Tsiodras, S., Tsakris, A., Dimopoulos, M.-A. and Thomaidis, N.S. 2021. Analytical methodologies for the detection of SARS-CoV-2 in wastewater: Protocols and future perspectives. *TrAC Trends in Analytical Chemistry* 134, 116125.
- Amoah, I.D., Abunama, T., Awolusi, O.O., Pillay, L., Pillay, K., Kumari, S. and Bux, F. 2022. Effect of selected wastewater characteristics on estimation of SARS-CoV-2 viral load in wastewater. *Environmental Research* 203, 111877.
- Balboa, S., Mauricio-Iglesias, M., Rodriguez, S., Martínez-Lamas, L., Vasallo, F.J., Regueiro, B. and Lema, J.M. 2020. The fate of SARS-CoV-2 in WWTPs points out the sludge line as a suitable spot for monitoring. *medRxiv*, 2020.2005.2025.20112706.
- Barril, P.A., Pianciola, L.A., Mazzeo, M., Ousset, M.J., Jaureguiberry, M.V., Alessandrello, M., Sánchez, G. and Oteiza, J.M. 2021. Evaluation of viral concentration methods for SARS-CoV-2 recovery from wastewaters. *Sci Total Environ* 756, 144105-144105.
- Benefield, A.E., Skrip, L.A., Clement, A., Althouse, R.A., Chang, S. and Althouse, B.M. 2020. SARS-CoV-2 viral load peaks prior to symptom onset: a systematic review and individual-pooled analysis of coronavirus viral load from 66 studies. *medRxiv*, 2020.2009.2028.20202028.
- Bi, Q., Lessler, J., Eckerle, I., Lauer, S.A., Kaiser, L., Vuilleumier, N., Cummings, D.A.T., Flahault, A., Petrovic, D., Guessous, I., Stringhini, S. and Azman, A.S. 2021. Household Transmission of SARS-CoV-2: Insights from a Population-based Serological Survey. *medRxiv*, 2020.2011.2004.20225573.
- Bishop, N., Jones-Lepp, T., Margetts, M., Sykes, J., Alvarez, D. and Keil, D.E. 2020. Wastewater-based epidemiology pilot study to examine drug use in the Western United States. *Sci Total Environ* 745, 140697-140697.
- Bisseux, M., Colombet, J., Mirand, A., Roque-Afonso, A.M., Abravanel, F., Izopet, J., Archimbaud, C., Peigue-Lafeuille, H., Debros, D., Bailly, J.L. and Henquell, C. 2018.

Monitoring human enteric viruses in wastewater and relevance to infections encountered in the clinical setting: a one-year experiment in central France, 2014 to 2015. *Euro Surveill* 23(7).

- Bivins, A., Greaves, J., Fischer, R., Yinda, K.C., Ahmed, W., Kitajima, M., Munster, V.J. and Bibby, K. 2020a. Persistence of SARS-CoV-2 in Water and Wastewater. *Environmental Science & Technology Letters* 7(12), 937-942.
- Bivins, A., North, D., Ahmad, A., Ahmed, W., Alm, E., Been, F., Bhattacharya, P., Bijlsma, L., Boehm, A.B., Brown, J., Buttiglieri, G., Calabro, V., Carducci, A., Castiglioni, S., Cetecioglu Gurol, Z., Chakraborty, S., Costa, F., Curcio, S., de los Reyes, F.L., Delgado Vela, J., Farkas, K., Fernandez-Casi, X., Gerba, C., Gerrity, D., Girones, R., Gonzalez, R., Haramoto, E., Harris, A., Holden, P.A., Islam, M.T., Jones, D.L., Kasprzyk-Hordern, B., Kitajima, M., Kotlarz, N., Kumar, M., Kuroda, K., La Rosa, G., Malpei, F., Mautus, M., McLellan, S.L., Medema, G., Meschke, J.S., Mueller, J., Newton, R.J., Nilsson, D., Noble, R.T., van Nuijs, A., Peccia, J., Perkins, T.A., Pickering, A.J., Rose, J., Sanchez, G., Smith, A., Stadler, L., Stauber, C., Thomas, K., van der Voorn, T., Wigginton, K., Zhu, K. and Bibby, K. 2020b. Wastewater-Based Epidemiology: Global Collaborative to Maximize Contributions in the Fight Against COVID-19. *Environmental Science & Technology* 54(13), 7754-7757.
- Bustin, S.A., Benes, V., Garson, J.A., Hellems, J., Huggett, J., Kubista, M., Mueller, R., Nolan, T., Pfaffl, M.W., Shipley, G.L., Vandesompele, J. and Wittwer, C.T. 2009. The MIQE Guidelines: Minimum Information for Publication of Quantitative Real-Time PCR Experiments. *Clinical Chemistry* 55(4), 611-622.
- Calgua, B., Mengewein, A., Grunert, A., Bofill-Mas, S., Clemente-Casares, P., Hundesa, A., Wyn-Jones, A.P., López-Pila, J.M. and Girones, R. 2008. Development and application of a one-step low cost procedure to concentrate viruses from seawater samples. *J Virol Methods* 153(2), 79-83.
- Carducci, A., Federigi, I., Liu, D., Thompson, J.R. and Verani, M. 2020. Making Waves: Coronavirus detection, presence and persistence in the water environment: State of the art and knowledge needs for public health. *Water Res* 179, 115907.
- CDC 2020 2019-Novel Coronavirus (2019-nCoV) Real-time rRT-PCR Panel
- Primers and Probes
- Chen, C., Hayward, K., Khan, S.J., Örmeci, B., Pillay, S., Rose, J.B., Thanikal, J.V. and Zhang, T. 2021. Role of wastewater treatment in COVID-19 control. *Water Quality Research Journal* 56(2), 68-82.
- Chen, Y., Chen, L., Deng, Q., Zhang, G., Wu, K., Ni, L., Yang, Y., Liu, B., Wang, W., Wei, C., Yang, J., Ye, G. and Cheng, Z. 2020. The presence of SARS-CoV-2 RNA in the feces of COVID-19 patients. *Journal of Medical Virology* 92(7), 833-840.
- Chik, A.H.S., Glier, M.B., Servos, M., Mangat, C.S., Pang, X.-L., Qiu, Y., D'Aoust, P.M., Burnet, J.-B., Delatolla, R., Dorner, S., Geng, Q., Giesy, J.P., McKay, R.M., Mulvey, M.R., Prystajecy, N., Srikanthan, N., Xie, Y., Conant, B. and Hruday, S.E. 2021. Comparison of approaches to quantify SARS-CoV-2 in wastewater using RT-qPCR: Results and implications from a collaborative inter-laboratory study in Canada. *Journal of Environmental Sciences* 107, 218-229.
- D'Aoust, P.M., Mercier, E., Montpetit, D., Jia, J.J., Alexandrov, I., Neault, N., Baig, A.T., Mayne, J., Zhang, X., Alain, T., Langlois, M.A., Servos, M.R., MacKenzie, M., Figeys, D., MacKenzie, A.E., Graber, T.E. and Delatolla, R. 2021. Quantitative analysis of SARS-

- CoV-2 RNA from wastewater solids in communities with low COVID-19 incidence and prevalence. *Water Res* 188, 116560.
- Day, M. 2020. Covid-19: identifying and isolating asymptomatic people helped eliminate virus in Italian village. *BMJ* 368, m1165.
- Diemert, S. and Yan, T. 2020. Municipal Wastewater Surveillance Revealed a High Community Disease Burden of a Rarely Reported and Possibly Subclinical Salmonella enterica Serovar Derby Strain. *Appl Environ Microbiol* 86(17).
- Eveleigh, D., Lloyd, M. and Hui, F. 2019 Using Armored RNA<sup>®</sup>/DNA as Reliable Molecular Controls in Infectious Disease Testing and Beyond, Asuragen Inc.
- Gerrity, D., Papp, K., Stoker, M., Sims, A. and Frehner, W. 2021. Early-pandemic wastewater surveillance of SARS-CoV-2 in Southern Nevada: Methodology, occurrence, and incidence/prevalence considerations. *Water Research X* 10, 100086.
- Graham, K.E., Loeb, S.K., Wolfe, M.K., Catoe, D., Sinnott-Armstrong, N., Kim, S., Yamahara, K.M., Sassoubre, L.M., Mendoza Grijalva, L.M., Roldan-Hernandez, L., Langenfeld, K., Wigginton, K.R. and Boehm, A.B. 2021. SARS-CoV-2 RNA in Wastewater Settled Solids Is Associated with COVID-19 Cases in a Large Urban Sewershed. *Environmental Science & Technology* 55(1), 488-498.
- Guan, W.-j., Ni, Z.-y., Hu, Y., Liang, W.-h., Ou, C.-q., He, J.-x., Liu, L., Shan, H., Lei, C.-l., Hui, D.S.C., Du, B., Li, L.-j., Zeng, G., Yuen, K.-Y., Chen, R.-c., Tang, C.-l., Wang, T., Chen, P.-y., Xiang, J., Li, S.-y., Wang, J.-l., Liang, Z.-j., Peng, Y.-x., Wei, L., Liu, Y., Hu, Y.-h., Peng, P., Wang, J.-m., Liu, J.-y., Chen, Z., Li, G., Zheng, Z.-j., Qiu, S.-q., Luo, J., Ye, C.-j., Zhu, S.-y. and Zhong, N.-s. 2020. Clinical Characteristics of Coronavirus Disease 2019 in China. *New England Journal of Medicine* 382(18), 1708-1720.
- Gupta, S., Parker, J., Smits, S., Underwood, J. and Dolwani, S. 2020. Persistent viral shedding of SARS-CoV-2 in faeces - a rapid review. *Colorectal Dis* 22(6), 611-620.
- Haramoto, E., Malla, B., Thakali, O. and Kitajima, M. 2020. First environmental surveillance for the presence of SARS-CoV-2 RNA in wastewater and river water in Japan. *Sci Total Environ* 737, 140405-140405.
- Hasan, S.W., Ibrahim, Y., Daou, M., Kannout, H., Jan, N., Lopes, A., Alsafar, H. and Yousef, A.F. 2021. Detection and quantification of SARS-CoV-2 RNA in wastewater and treated effluents: Surveillance of COVID-19 epidemic in the United Arab Emirates. *Science of The Total Environment* 764, 142929.
- Havers, F.P., Reed, C., Lim, T., Montgomery, J.M., Klena, J.D., Hall, A.J., Fry, A.M., Cannon, D.L., Chiang, C.-F., Gibbons, A., Krapiunaya, I., Morales-Betoulle, M., Roguski, K., Rasheed, M.A.U., Freeman, B., Lester, S., Mills, L., Carroll, D.S., Owen, S.M., Johnson, J.A., Semenova, V., Blackmore, C., Blog, D., Chai, S.J., Dunn, A., Hand, J., Jain, S., Lindquist, S., Lynfield, R., Pritchard, S., Sokol, T., Sosa, L., Turabelidze, G., Watkins, S.M., Wiesman, J., Williams, R.W., Yendell, S., Schiffer, J. and Thornburg, N.J. 2020. Seroprevalence of Antibodies to SARS-CoV-2 in 10 Sites in the United States, March 23-May 12, 2020. *JAMA Internal Medicine* 180(12), 1576-1586.
- He, X., Lau, E.H.Y., Wu, P., Deng, X., Wang, J., Hao, X., Lau, Y.C., Wong, J.Y., Guan, Y., Tan, X., Mo, X., Chen, Y., Liao, B., Chen, W., Hu, F., Zhang, Q., Zhong, M., Wu, Y., Zhao, L., Zhang, F., Cowling, B.J., Li, F. and Leung, G.M. 2020. Temporal dynamics in viral shedding and transmissibility of COVID-19. *Nature Medicine* 26(5), 672-675.
- Hietala, S.K. and Crossley, B.M. 2006. Armored RNA as virus surrogate in a real-time reverse transcriptase PCR assay proficiency panel. *J Clin Microbiol* 44(1), 67-70.

- Hill, K., Zamyadi, A., Deere, D., Vanrolleghem, P.A. and Crosbie, N.D. 2020. SARS-CoV-2 known and unknowns, implications for the water sector and wastewater-based epidemiology to support national responses worldwide: early review of global experiences with the COVID-19 pandemic. *Water Quality Research Journal*.
- Hoffmann, T. and Alsing, J. 2021. Faecal shedding models for SARS-CoV-2 RNA amongst hospitalised patients and implications for wastewater-based epidemiology. medRxiv, 2021.2003.2016.21253603.
- Hokajärvi, A.-M., Rytönen, A., Tiwari, A., Kauppinen, A., Oikarinen, S., Lehto, K.-M., Kankaanpää, A., Gunnar, T., Al-Hello, H., Blomqvist, S., Miettinen, I.T., Savolainen-Kopra, C. and Pitkänen, T. 2021a. The detection and stability of the SARS-CoV-2 RNA biomarkers in wastewater influent in Helsinki, Finland. *Science of The Total Environment* 770, 145274.
- Hokajärvi, A.M., Rytönen, A., Tiwari, A., Kauppinen, A., Oikarinen, S., Lehto, K.M., Kankaanpää, A., Gunnar, T., Al-Hello, H., Blomqvist, S., Miettinen, I.T., Savolainen-Kopra, C. and Pitkänen, T. 2021b. The detection and stability of the SARS-CoV-2 RNA biomarkers in wastewater influent in Helsinki, Finland. *Sci Total Environ* 770, 145274.
- Hong, P.Y., Rachmadi, A.T., Mantilla-Calderon, D., Alkahtani, M., Bashawri, Y.M., Al Qarni, H., O'Reilly, K.M. and Zhou, J. 2021. Estimating the minimum number of SARS-CoV-2 infected cases needed to detect viral RNA in wastewater: To what extent of the outbreak can surveillance of wastewater tell us? *Environ Res* 195, 110748.
- Ing, A.J., Cocks, C. and Green, J.P. 2020. COVID-19: in the footsteps of Ernest Shackleton. *Thorax* 75(8), 693.
- Ivanova, O.E., Yarmolskaya, M.S., Eremeeva, T.P., Babkina, G.M., Baykova, O.Y., Akhmadishina, L.V., Krasota, A.Y., Kozlovskaya, L.I. and Lukashev, A.N. 2019. Environmental Surveillance for Poliovirus and Other Enteroviruses: Long-Term Experience in Moscow, Russian Federation, 2004–2017. *Viruses* 11(5), 424.
- Jones, D.L., Baluja, M.Q., Graham, D.W., Corbishley, A., McDonald, J.E., Malham, S.K., Hillary, L.S., Connor, T.R., Gaze, W.H., Moura, I.B., Wilcox, M.H. and Farkas, K. 2020. Shedding of SARS-CoV-2 in feces and urine and its potential role in person-to-person transmission and the environment-based spread of COVID-19. *Sci Total Environ* 749, 141364.
- Kitajima, M., Ahmed, W., Bibby, K., Carducci, A., Gerba, C.P., Hamilton, K.A., Haramoto, E. and Rose, J.B. 2020. SARS-CoV-2 in wastewater: State of the knowledge and research needs. *Science of The Total Environment* 739, 139076.
- Lauer, S.A., Grantz, K.H., Bi, Q., Jones, F.K., Zheng, Q., Meredith, H.R., Azman, A.S., Reich, N.G. and Lessler, J. 2020. The Incubation Period of Coronavirus Disease 2019 (COVID-19) From Publicly Reported Confirmed Cases: Estimation and Application. *Annals of Internal Medicine* 172(9), 577-582.
- Li, Q., Guan, X., Wu, P., Wang, X., Zhou, L., Tong, Y., Ren, R., Leung, K.S.M., Lau, E.H.Y., Wong, J.Y., Xing, X., Xiang, N., Wu, Y., Li, C., Chen, Q., Li, D., Liu, T., Zhao, J., Liu, M., Tu, W., Chen, C., Jin, L., Yang, R., Wang, Q., Zhou, S., Wang, R., Liu, H., Luo, Y., Liu, Y., Shao, G., Li, H., Tao, Z., Yang, Y., Deng, Z., Liu, B., Ma, Z., Zhang, Y., Shi, G., Lam, T.T.Y., Wu, J.T., Gao, G.F., Cowling, B.J., Yang, B., Leung, G.M. and Feng, Z. 2020. Early Transmission Dynamics in Wuhan, China, of Novel Coronavirus–Infected Pneumonia. *New England Journal of Medicine* 382(13), 1199-1207.

- Manitoba, G.o. 2021 Manitoba COVID-19, <https://experience.arcgis.com/experience/f55693e56018406ebbd08b3492e99771>, <https://experience.arcgis.com/experience/f55693e56018406ebbd08b3492e99771>.
- Markt, R., Mayr, M., Peer, E., Wagner, A.O., Lackner, N. and Insam, H. 2021. Detection and stability of SARS-CoV-2 fragments in wastewater: Impact of storage temperature. medRxiv, 2021.2002.2022.21250768.
- McCall, C., Wu, H., Miyani, B. and Xagorarakis, I. 2020. Identification of multiple potential viral diseases in a large urban center using wastewater surveillance. *Water Res* 184, 116160.
- Medema, G., Heijnen, L., Elsinga, G., Italiaander, R. and Brouwer, A. 2020a. Presence of SARS-Coronavirus-2 in sewage. medRxiv, 2020.2003.2029.20045880.
- Medema, G., Heijnen, L., Elsinga, G., Italiaander, R. and Brouwer, A. 2020b. Presence of SARS-Coronavirus-2 RNA in Sewage and Correlation with Reported COVID-19 Prevalence in the Early Stage of the Epidemic in The Netherlands. *Environmental Science & Technology Letters* 7(7), 511-516.
- Nakamura, T., Hamasaki, M., Yoshitomi, H., Ishibashi, T., Yoshiyama, C., Maeda, E., Sera, N. and Yoshida, H. 2015. Environmental surveillance of poliovirus in sewage water around the introduction period for inactivated polio vaccine in Japan. *Appl Environ Microbiol* 81(5), 1859-1864.
- Pan, Y., Zhang, D., Yang, P., Poon, L.L.M. and Wang, Q. 2020. Viral load of SARS-CoV-2 in clinical samples. *The Lancet Infectious Diseases* 20(4), 411-412.
- Parsa, S.M., Momeni, S., Hemmat, A. and Afrand, M. 2021. Effectiveness of solar water disinfection in the era of COVID-19 (SARS-CoV-2) pandemic for contaminated water/wastewater treatment considering UV effect and temperature. *Journal of Water Process Engineering* 43, 102224.
- Peccia, J., Zulli, A., Brackney, D.E., Grubaugh, N.D., Kaplan, E.H., Casanovas-Massana, A., Ko, A.I., Malik, A.A., Wang, D., Wang, M., Warren, J.L., Weinberger, D.M., Arnold, W. and Omer, S.B. 2020. Measurement of SARS-CoV-2 RNA in wastewater tracks community infection dynamics. *Nature Biotechnology* 38(10), 1164-1167.
- Philo, S.E., Keim, E.K., Swanstrom, R., Ong, A.Q.W., Burnor, E.A., Kossik, A.L., Harrison, J.C., Demeke, B.A., Zhou, N.A., Beck, N.K., Shirai, J.H. and Meschke, J.S. 2021. A comparison of SARS-CoV-2 wastewater concentration methods for environmental surveillance. *Science of The Total Environment* 760, 144215.
- Randazzo, W., Truchado, P., Cuevas-Ferrando, E., Simón, P., Allende, A. and Sánchez, G. 2020. SARS-CoV-2 RNA in wastewater anticipated COVID-19 occurrence in a low prevalence area. *Water Res* 181, 115942-115942.
- Saawarn, B. and Hait, S. 2021. Occurrence, fate and removal of SARS-CoV-2 in wastewater: Current knowledge and future perspectives. *J Environ Chem Eng* 9(1), 104870-104870.
- Sherchan, S.P., Shahin, S., Ward, L.M., Tandukar, S., Aw, T.G., Schmitz, B., Ahmed, W. and Kitajima, M. 2020. First detection of SARS-CoV-2 RNA in wastewater in North America: A study in Louisiana, USA. *Sci Total Environ* 743, 140621-140621.
- Simpson, A., Topol, A., White, B.J., Wolfe, M.K., Wigginton, K.R. and Boehm, A.B. 2021. Effect of storage conditions on SARS-CoV-2 RNA quantification in wastewater solids. *PeerJ* 9, e11933.
- Sulej-Suchomska, A.M., Klupczynska, A., Dereziński, P., Matysiak, J., Przybyłowski, P. and Kokot, Z.J. 2020. Urban wastewater analysis as an effective tool for monitoring



- illegal drugs, including new psychoactive substances, in the Eastern European region. *Scientific Reports* 10(1), 4885.
- Thompson, J.R., Nanchaiah, Y.V., Gu, X., Lee, W.L., Rajal, V.B., Haines, M.B., Girones, R., Ng, L.C., Alm, E.J. and Wuertz, S. 2020. Making waves: Wastewater surveillance of SARS-CoV-2 for population-based health management. *Water Res* 184, 116181-116181.
- Uyaguari-Diaz, M.I., Chan, M., Chaban, B.L., Croxen, M.A., Finke, J.F., Hill, J.E., Peabody, M.A., Van Rossum, T., Suttle, C.A., Brinkman, F.S.L., Isaac-Renton, J., Prystajek, N.A. and Tang, P. 2016. A comprehensive method for amplicon-based and metagenomic characterization of viruses, bacteria, and eukaryotes in freshwater samples. *Microbiome* 4(1), 20.
- Wei, W.E., Li, Z., Chiew, C.J., Yong, S.E., Toh, M.P. and Lee, V.J. 2020. Presymptomatic Transmission of SARS-CoV-2 - Singapore, January 23-March 16, 2020. *MMWR Morb Mortal Wkly Rep* 69(14), 411-415.
- Westhaus, S., Weber, F.-A., Schiwy, S., Linnemann, V., Brinkmann, M., Widera, M., Greve, C., Janke, A., Hollert, H., Wintgens, T. and Ciesek, S. 2021. Detection of SARS-CoV-2 in raw and treated wastewater in Germany – Suitability for COVID-19 surveillance and potential transmission risks. *Science of The Total Environment* 751, 141750.
- Winnipeg, T.C.o. 2021 Population of Winnipeg, The City of Winnipeg, <https://winnipeg.ca/cao/pdfs/population.pdf>.
- Wölfel, R., Corman, V.M., Guggemos, W., Seilmaier, M., Zange, S., Müller, M.A., Niemeyer, D., Jones, T.C., Vollmar, P., Rothe, C., Hoelscher, M., Bleicker, T., Brünink, S., Schneider, J., Ehmann, R., Zwirgmaier, K., Drosten, C. and Wendtner, C. 2020. Virological assessment of hospitalized patients with COVID-2019. *Nature* 581(7809), 465-469.
- Wu, F., Xiao, A., Zhang, J., Moniz, K., Endo, N., Armas, F., Bonneau, R., Brown, M.A., Bushman, M., Chai, P.R., Duvallet, C., Erickson, T.B., Foppe, K., Ghaeli, N., Gu, X., Hanage, W.P., Huang, K.H., Lee, W.L., Matus, M., McElroy, K.A., Nagler, J., Rhode, S.F., Santillana, M., Tucker, J.A., Wuertz, S., Zhao, S., Thompson, J. and Alm, E.J. 2022. SARS-CoV-2 RNA concentrations in wastewater foreshadow dynamics and clinical presentation of new COVID-19 cases. *Science of The Total Environment* 805, 150121.
- Wu, S.L., Mertens, A.N., Crider, Y.S., Nguyen, A., Pokpongkiat, N.N., Djajadi, S., Seth, A., Hsiang, M.S., Colford, J.M., Reingold, A., Arnold, B.F., Hubbard, A. and Benjamin-Chung, J. 2020. Substantial underestimation of SARS-CoV-2 infection in the United States. *Nature Communications* 11(1), 4507.
- Yan, T., O'Brien, P., Shelton, J.M., Whelen, A.C. and Pagaling, E. 2018. Municipal Wastewater as a Microbial Surveillance Platform for Enteric Diseases: A Case Study for Salmonella and Salmonellosis. *Environmental Science & Technology* 52(8), 4869-4877.
- Ye, Y., Ellenberg, R.M., Graham, K.E. and Wigginton, K.R. 2016. Survivability, Partitioning, and Recovery of Enveloped Viruses in Untreated Municipal Wastewater. *Environmental Science & Technology* 50(10), 5077-5085.